# A prolyl oligopeptidase inhibitor, KYP-2047, reduces $\alpha$-synuclein protein levels and aggregates in cellular and animal models of Parkinson's disease

# A prolyl oligopeptidase inhibitor, KYP-2047, reduces α-synuclein protein levels and aggregates in cellular and animal models of Parkinson's disease

Running title: PREP inhibitor reduces α-synuclein levels

T T Myöhänen*[5], M J Hannula[5], R Van Elzen[1], M Gerard[2], P Van Der Veken[3], J A García-Horsman[5], V Baekelandt[4], P T Männistö[5], A M Lambeir[1]

[1] Laboratory of Medical Biochemistry, University of Antwerp, B-2610, Wilrijk (Antwerp), Belgium

[2] Laboratory of Biochemistry, Katholieke Universiteit Leuven-Kortrijk, B-8500, Belgium

[3] Laboratory of Medicinal Chemistry, University of Antwerp, B-2610, Wilrijk (Antwerp), Belgium

[4] Laboratory for Neurobiology and Gene Therapy, Division of Molecular Medicine, Katholieke Universiteit Leuven, B-3000 Leuven, Belgium

[5] Division of Pharmacology and Toxicology, FI-00014, University of Helsinki, Finland

***Corresponding author:** Timo T. Myöhänen, Division of Pharmacology and Toxicology, Faculty of Pharmacy, University of Helsinki, P.O. Box 56 (Viikinkaari 5E), FI-00014 University of Helsinki, Finland. Tel. +358-9-191 59478, Fax. +358-9-191 59471, E-mail: Timo.Myöhänen@helsinki.fi

This is an Accepted Article that has been peer-reviewed and approved for publication in the *British Journal of Pharmacology*, but has yet to undergo copyediting and proof correction. Please cite this article as an "Accepted Article"; doi: 10.1111/j.1476-5381.2012.01846.x

**Abstract**

*Background and purpose:* The aggregation of α-synuclein (α-syn) is connected to the pathology of Parkinson's disease. Recently, it was shown that prolyl oligopeptidase (PREP) accelerates the aggregation of α-syn *in vitro*. The aim of this study was to investigate the effects of a PREP inhibitor, KYP-2047, on α-syn aggregation in cell lines overexpressing wild-type or A30P/A53T mutant human α-syn, and in the brains of two A30P α-syn transgenic mouse strains.

*Experimental approach:* Cells were exposed to oxidative stress, and then incubated with the PREP inhibitor during or after the stress. Wild-type or transgenic mice were treated for 5 days with KYP-2047 (2x3 mg/kg a day). Besides immunohistochemistry and thioflavin S staining, soluble and insoluble α-syn protein levels were measured by Western blot. α-syn mRNA levels were quantified by PCR. The colocalization of PREP and α-syn, and the effect of KYP-2047 on cell viability were also investigated.

*Key results:* In cell lines, oxidative stress induced a robust aggregation of α-syn, and low concentrations of KYP-2047 significantly reduced the number of cells with α-syn inclusions while abolishing the colocalization of α-syn and PREP. KYP-2047 significantly reduced the amount of aggregated α-syn, and it had beneficial effects on cell viability. In the transgenic mice, a 5-day treatment with the PREP inhibitor reduced the amount of α-syn immunoreactivity and soluble α-syn protein in the brain.

*Conclusions and implications:* The results suggest that the PREP may play a role in brain accumulation and aggregation of α-syn, while KYP-2047 seems to effectively prevent these processes.

**Keywords:** Serine protease, prolyl oligopeptidase inhibitor, α-synuclein, Parkinson's disease, protein aggregation

**Abbreviations:** AMC, amino methyl coumarin; α-syn, α-synuclein; DMEM, Dulbecco's Modified Eagle Medium; FBS, fetal bovine serum; IHC, immunohistochemistry; KYP-2047, 4-phenylbutanoyl-*L*-prolyl-2(*S*)-cyanopyrrolidine; NEAA, non-essential amino acids; PREP, prolyl oligopeptidase; WB, Western blot; WT, wild-type.

## Introduction

α-Synuclein (α-syn) is a 140 amino acid sized cytosolic brain protein of the synuclein family. It interacts with membranes and vesicles, and is found also in the nucleus (McLean *et al.,* 2000; Yu *et al.,* 2007; Surguchov 2008). Several physiological functions have been suggested for α-syn, including synaptic transmission, axonal transport, and the regulation of dopamine release (for reviews, see Surguchov 2008; Bisaglia *et al.,* 2009).

Insoluble fibrillar inclusions of α-syn have been identified as the main component of Lewy bodies in Parkinson's disease (PD) and Lewy body dementia, concomitant with neuronal death and clinical symptoms (Spillantini *et al.,* 1997; Arima *et al.,* 1998; Surguchov 2008). Further clinical evidence for the importance of α-syn in PD is derived from mutations in the α-syn gene. Duplication or triplication, or three missense mutations in the α-syn gene, producing the changes A30P, A53T and E46K in the protein, have been identified as the cause of early-onset autosomal dominant familial PD (Polymeropoulos *et al.,* 1997; Kruger *et al.,* 1998; Singleton *et al.*, 2003; Ibanez *et al.,* 2004; Singleton *et al.*, 2004; Zarranz *et al.,* 2004).

The aggregation of α-syn is a nucleation-dependent polymerization process (Wood *et al.,* 1999). Several factors increasing the nucleation and aggregation of α-syn have been identified, including oxidative stress, low pH, increased ionic strength and defects in protein trafficking and processing (Uversky *et al.,* 2001; Cooper *et al.,* 2006; Kim *et al.,* 2008). Recently, it was shown that enzymes

of the FK506 binding protein family increase the aggregation of α-syn *in vitro* and *in vivo* (Gerard *et al.,* 2008; Gerard *et al.,* 2010; Deleersnijder *et al.,* 2011). Moreover, a serine protease, prolyl oligopeptidase (PREP; POP; PO; EC 3.4.21.26), accelerates and increases the aggregation of wild-type (WT) α-syn under cell-free conditions, possibly by increasing the nucleation rate (Brandt *et al.,* 2008; Lambeir 2011). Interestingly, this action can be blocked by PREP inhibitors or by PREP active site mutation.

PREP is present in different species and, in mammals, it is widely distributed in the tissues, hydrolyzing bioactive peptides of less than 30 amino acids at the carboxyl side of proline residue (for review, see Garcia-Horsman *et al.,* 2007). Alterations in PREP enzyme activity have been measured in several diseases, including PD and Lewy body dementia (Mantle *et al.,* 1996). These findings combined with earlier reports of anti-amnesic effects (Yoshimoto *et al.,* 1987) have served as the rationale for developing PREP inhibitors to combat neurodegenerative diseases via restoring low neuropeptide levels. Several potent substrate-like PREP inhibitors have been developed, and extensively characterized. Although some beneficial effects in animal memory models (Yoshimoto *et al.,* 1987; Toide *et al.,* 1997; Shishido *et al.,* 1998) and in senescence accelerated mice (Kato *et al.,* 1997) have been reported, the *in vivo* results of PREP inhibitors are rather controversial (for review, see Männistö *et al.,* 2007). Recent studies have suggested that PREP has other actions beyond its peptidase activity, relying on protein-protein interactions (Brandt *et al.,* 2008; Di Daniel *et al.,* 2009; Myöhänen *et al.,* 2010a).

To further clarify the role of PREP in α-syn aggregation, we tested the effect of a PREP inhibitor on α-syn aggregation *in vitro,* in several cell lines overexpressing different forms of α-syn, and *in vivo,* in two mouse strains overexpressing α-syn with the pathogenic A30P mutation. As a conclusion, in this study we have revealed that a PREP inhibitor, KYP-2047 (4-phenylbutanoyl-*L*-prolyl-2(*S*)-cyanopyrrolidine), is effective in preventing the formation of α-syn aggregates in α-syn overexpressing cell lines, possibly via abolishing the colocalization between PREP and α-syn.

Moreover, KYP-2047 accelerates the clearance of α-syn aggregates after oxidative stress in cells, and reduces the soluble and insoluble α-syn protein levels in overexpressing cellular and *in vivo* models. Further, based on these results, it can be hypothesized that besides nucleation, PREP may influence on α-syn aggregation process with some other mechanisms, e.g. by affecting aggresomal processing of misfolding proteins.

## METHODS

### Chemicals

Chemicals were purchased from Sigma-Aldrich (St. Louis, MO, USA) unless otherwise specified in the text. The PREP inhibitor, KYP-2047, was synthesized as previously described (Jarho *et al.,* 2004). KYP-2047 was chosen as a reference compound since the biochemical and pharmacological data indicate it is potent and selective, that it enters SH-SY5Y cells in culture and crosses the blood-brain barrier effectively in rodents (Jarho *et al.,* 2004; Venäläinen *et al.,* 2006; Jalkanen *et al.,* 2007; Jalkanen *et al.,* 2011). The drug/molecular target nomenclature conforms to BJP's Guide to Receptors and Channels (Alexander *et al*., 2009)

### Antibodies

Commercial antibodies were chosen carefully taking into account that the manufacturer provided a proof of quality based on publications in which the production and specificity of the antibodies have been properly validated. See details and dilutions of primary antibodies in Table 1.

**Cell lines**

WT SH-SY5Y human neuroblastoma cell line was purchased from ATCC (LGC Standards; Product # CRL-2266, Middlesex, UK). Cells were cultured with Dulbecco's modified eagle medium (DMEM-Glutamax, Product# 31966-021; Invitrogen/Gibco, Paisley, UK) containing 15% fetal bovine serum (FBS, Product# 16000-044; Invitrogen/Gibco), 1% non-essential amino acids (NEAA, Product# 11140; Invitrogen/Gibco) and 50 µg/ml Gentamycin (Product# 15750-094; Invitrogen/Gibco).

Stable cell lines expressing WT, A30P and A53T a-syn were generated using a lentiviral vector as described in Gerard *et al.,* (2010) and transfected cells were selected by puromycin resistance. α-syn overexpressing cells were cultured with DMEM-Glutamax (Invitrogen/Gibco) containing 15% FBS (Invitrogen/Gibco), 1% NEAA (Invitrogen/Gibco), 50 µg/ml gentamycin (Invitrogen/Gibco) and 1 µg/ml puromycin (Invitrogen/Gibco). Cell lines were used at passages 3 to 15 and grown at 37°C and 5% $CO_2$ in a humidified atmosphere.

**Induction of α-synuclein aggregation by oxidative stress and the effect of KYP-2047**

Cells were seeded in 12-well-plates or T25-flasks and allowed to grow overnight. The number of cells was assay dependent (see amounts below). Thereafter, the aggregation process of α-syn was induced by adding 100 µM $H_2O_2$ and 10 mM $FeCl_2$ in cell culturing medium for 3 days as described (Gerard *et al.,* 2010). The following groups were formed to test the effects of KYP-2047 on α-syn aggregation in cells : 1) Oxidative stress 3 days with 0.001% DMSO (Stress 3d with veh); 2) Oxidative stress 3 days with 1 µM KYP-2047 in 0.001% DMSO (Stress 3d with KYP); 3) medium 3 days (negative control); 4) 1 µM KYP-2047 in 0.001% DMSO 3 days (KYP 3d); 5) 0.001% DMSO 3 days (Veh 3d); 6) Oxidative stress 3 days (Stress 3d). The concentration-response of KYP-2047 was tested with various concentrations (1 nM, 1 µM, 10 µM and 100 µM) in Stress 3d experiments for A30P and A53T cell lines.

To test if the outcome is dependent on antioxidant effects of KYP-2047 during the induction of oxidative stress, an experiment was performed where KYP-2047 and vehicle/medium control were added for 1 day following the 3 days of oxidative stress with the same concentrations as in the Stress 3d experiment described above.

**Cell immunofluorescence**

The effect of oxidative stress and KYP-2047 on α-syn aggregation in cells was studied using immunofluorescence by a modification of the protocol by Gerard et al. (2010). Briefly, cells were seeded in 12 well-plates with coverslips (Nunc, Roskilde, Denmark) at a density of 500,000 cells/ml and allowed to grow in medium for 24 h. Thereafter, the aggregation of α-syn was induced by oxidative stress as described above. After treatment and fixation of the cells with 4% paraformaldehyde solution, unspecific binding was blocked by incubation of 30 min with 10% Normal Goat Serum for α-syn (NGS, Product# S-1000; Vector Laboratories, Burlinge, CA, USA) and with 10% Normal Rabbit Serum for PREP (NRS, Product# S-5000; Vector Laboratories) in PBS, pH 7.4. Primary antibodies were added (see Table 1) and incubated overnight at room temperature. After washing with PBS, 2 h incubation with secondary antibody followed. (1:500 goat anti-mouse fluorescein conjugated for α-syn, Product# 31966, Thermo Fisher Scientific; 1:500 rabbit anti-chicken Texas Red conjugated for PREP, Product# ab6751, AbCam) Wavelengths for fluorescein were 494 nm (excitation) and 512 (emission), and for Texas Red 596 nm and 620 nm, respectively. The coverslips were mounted on slides using Vectashield with 4',6-diamidino-2-phenylindole (DAPI) (Product# H-1200, Vector Laboratories) as a nuclear marker (wavelengths 358 nm (excitation) and 461 nm (emission)). Control stainings for the immunofluorescence protocol were carried out by omission of primary antibody. No evidence of any staining was observed in these negative controls (data not shown).

Immunofluorescence photomicrographs were captured by a digital camera connected to a microscope (Olympus BX61 microscope and DP40 Digital Camera, Olympus Corporation, Tokyo, Japan). Part of the sections were photographed using Leica TCS SP2 AOBS (Leica Microsystems Inc.) equipped with an argon-He/Ne laser mounted on an inverted Leica DM IRE2 microscope (Leica Microsystems Inc.). Minor corrections to brightness and contrast were made with Adobe Photoshop CS2 software (version 9.0, Adobe Systems Incorporated, Mountain View, CA, USA).

**α-syn fractionation and Western blotting (WB)**

To separate soluble and insoluble fractions of α-syn, the method described in Feng *et al.,* (2010) was used. Briefly, $1*10^6$ cells were seeded to T-25 flasks, and oxidative stress and study groups were prepared as described above. Cells were first lysed and mechanically homogenized on ice in modified RIPA buffer (50 mM Tris HCl pH 7.4, 1% NP-40, 0.25% sodium deoxycholate, 150 mM NaCl) with protease inhibitor cocktail (Product# P8340), phenylmethanesulfonyl fluoride (PMSF, Product# P7626) and Halt Phosphatase Inhibitor (Product# 87786, Thermo Fisher Scientific). After centrifuging at 13,300 rpm for 15 minutes at 4°C, supernatants (soluble fraction) were collected. Pellets were resuspended in denaturing sample buffer (62.5 mM Tris-HCl pH 6.8, 2% sodium dodecyl sulfate, 10% glycerol, 5% beta-mercaptoethanol and 0.001% bromophenol blue), boiled for 5 minutes and centrifuged as above for 1 minute. This fraction contained SDS-soluble monomers and oligomers of α-syn, and also SDS-resistant high molecular weight oligomers and aggregates. Protein levels were measured by using the method of Bradford (1976), and lysates were loaded on SDS-gel (12%) with equal protein amounts. Standard transfer and blocking techniques were used. For details of primary antibodies for α-syn, see Table 1. Horse anti-mouse HRP (dilution 1:2000 in 2% milk in TTBS (0.05% Tween20-TBS); Product #7076, Cell Signalling Technology, Danvers, MA, USA) was used as secondary antibody. The images were captured using GeneGnome (Syngene, Cambridge, UK). Three independent WB experiments were performed.

The levels of PREP in cell lines and brains of A30P transgenic mice were quantified by WB, modified from Myöhänen *et al.,* (2008b). The cells were homogenized as described above, tissues were homogenized in five volumes of assay buffer (0.1 M Na–K-phosphate buffer, pH 7.0), and the tissue homogenates were centrifuged at 16,000*g*, 4°C, for 20 min discarding the pellet. Standard SDS-PAGE (12%), transfer and blocking techniques were used, and β-actin served as the loading control. For details of primary antibodies for PREP and β-actin, see Table 1. For the α-syn and β-actin WB, goat anti-mouse secondary antibody with HRP conjugate (Product #31430, Thermo Fisher Scientific; dilution 1:5000 in 1% milk in TTBS was used. To detect PREP from cells and mice brain, rabbit anti-chicken HRP secondary antibody (Product #31401, Thermo Fisher Scientific; dilution 1:5000 in 1% milk in TTBS) was used. The images were captured using OptiGo (Isogen Life Sciences, De Meern, Netherlands). Three independent WB experiments were performed.

**Thioflavin S staining**

Thioflavin S staining of amyloid-type fibrils with beta structure was used as described earlier (Gerard *et al.,* 2010). Thioflavin S is a commonly used self-fluorescent marker of amyloid-type protein structure that binds also to α-syn aggregates (Conway et al., 2000). Briefly, cells were fixed for 15 min in 4% paraformaldehyde. After two PBS washes, cells were incubated with 0.05% Thioflavin S (Product# T1892) for 20 min, washed 2x5 min in 80% ethanol and 1x5 min in PBS, and covered with mounting medium (Vectashield; Product# H-1000, Vector Laboratories). Wavelengths for thioflavin S were 430 nm (excitation) and 550 nm (emission). Thioflavin S stained cells were photographed using a fluorescence microscope as described above.

**Double- label immunofluorescence**

Double-label immunofluorescence for α-syn and PREP markers was performed by modifying the protocol described earlier (Myöhänen *et al.,* 2008a). Briefly, after the α-syn staining, the slides were washed with PBS or TBS 3x5 min, incubated with 10% RBS, and thereafter PREP staining was done as described above (see antibodies in Table 1). Fluorescent double-labelled sections were photographed using an inverted microscope with laser scanning confocal device as described above, and the red channel was converted to magenta using Adobe Photoshop CS2 software (version 9.0, Adobe Systems Incorporated).

**Cell calculations**

The percentages of cells with cytosolic α-syn inclusions from immunofluorescence and thioflavin S stainings were calculated with Stereo Investigator software attached to Olympus BX61 microscope and DP40 Digital Camera (MBF Bioscience, Williston, VT, USA) by using the optical fractionator method (Lindholm *et al.,* 2007) and comparing the number of cells with clear and intense cytosolic α-syn expression to the total number of cells (see examples in Figs. 1 and 2). The α-syn inclusion-positive cell percentage for each condition was determined from 3 different experiments, each with two or three wells per condition and with 450-800 cells for each coverslip.

Colocalization percentages between PREP and α-syn were calculated as described (Myöhänen *et al.,* 2008a) without Abercrombie's correction since the cells grew in the monolayer. The colocalization percentage for each condition was calculated from 3 different experiments, each with two or three wells per condition and with 60-150 cells for each coverslip

**α-syn mRNA transcription levels**

Cells were grown in flasks and exposed to oxidative stress as described above. After 3 days , the cells were homogenized and the total RNA was extracted with Aurum Total RNA Mini Kit (Bio-Rad, Hercules, CA, USA) which includes DNase treatment. Reverse transcriptase reaction was done

on 100 ng of RNA in standard conditions using iScrpt™ cDNA Synthesis kit (Bio-Rad). PCR was performed with primers designed to amplify a fragment of α-syn cDNA (forward, AGG ACT TTC AAA GGC CAA GG; reverse. TCC TCC AAC ATT TGT CAC TTG C) or β-actin cDNA (forward. TCA CCA TGG ATG ATG ATA TCG CC; reverse. CCACAC GCA GCT CAT TGT AGA AGG), using iQ™ SYBR® Green Supermix (Bio-Rad).

After optimization of PCR conditions, amplification efficiency was evaluated for both α-syn and β-actin primers using four consecutive 10-fold dilutions of the cDNA. Determination was done in triplicate. The fold change of expression of α-syn, with respect to β-actin, is reported as $-2^{\Delta\Delta C(t)}$.

**PREP enzyme activity measurements**

In the cellular activity assays, the cells were seeded in T25-flasks at a density of $10^6$ cells/flask and, after 1 day incubation, were exposed to oxidative stress following the experimental set-up described above (6 groups). After 3 days, the cells were homogenized with lysis buffer (50 mM $KH_2PO_4$, 1.5 mM $MgCl_2$, 10 mM NaCl, 1mM EDTA; pH 7.4). Cell homogenates were centrifuged 16,000 g for 10 min in +4 °C, the supernatant was recovered and stored at -80 °C until use. PREP activity was measured from supernatants using Z-Gly-Pro-aminomethylcoumarine (AMC) substrate as described earlier (Moreno-Baylach *et al.,* 2008; Myöhänen *et al.,* 2008b). Total protein amounts were measured using the method of Bradford (Bradford 1976). All activity measurements were made in triplicate. The cell homogenates were also used in Western blot experiments. The same PREP activity assay was used also for mouse brain homogenates (see preparation below).

**Cell viability**

To assess the cell viability under oxidative stress, and the effect of KYP-2047 thereon, the LDH release assay, was used as described by Talman *et al.* (2011). Moreover, the effect of different dilutions of oxidative stress medium (see above; 100%, 75% and 50%) on cell viability and the

effect of KYP-2047 thereon were studied. In case of negative values in LDH assay, these values were set as 0% and other values were proportioned to this.

**Animals and tissue preparation**

As α-syn mouse model, we used Thy1–A30P–α-syn transgenic mice, where human A30P α-syn overexpression is driven by the Thy1 promoter as reported before (Kahle *et al.,* 2000). This transgenic mouse strain develops α-synucleinopathy in several brain regions, age-dependent cognitive decline after 12 months and progressive deterioration of locomotor function (Neumann *et al.,* 2002; Freichel *et al.,* 2007). Thy1-A30P-α-syn transgenic mice (16 males, weight 32-38 g, aged 59-72 weeks) and 13 WT control mice (C57BL/6 6JRccHsd, weigh 30-45 g, aged 62-68 weeks) were maintained under a 12:12 h light/dark cycle at temperature of 20-22°C. Food and water were available *ad libitum.* All animal procedures were conducted according to the Council of Europe (directive 86/609) guidelines, and approved by the Animal Ethics Committee of the University of Antwerp. The second A30P-α-syn transgenic mouse and the experiments performed on this strain are described in supplementary material.

Tissue processing for IHC and Western blot (WB) were performed by protocols described earlier (Myöhänen *et al.,* 2008a; Myöhänen *et al.,* 2008b). Briefly, animals were anesthetized with an overdose of pentobarbital (100 mg/kg; Orion Corporation, Espoo, Finland), and then perfused transcardially with PBS. The brains were then removed and dissected in two hemispheres; one hemisphere was fixed for IHC (4 + 18 h in 4% PFA) and the other one was frozen for WB analysis. Fixation, sectioning and homogenization were done as described earlier (Myöhänen *et al.,* 2008b).

**Treatment of A30P transgenic mice with a PREP inhibitor**

A30P transgenic mice were separated in two groups, a group treated with KYP-2047 (n = 7) and a vehicle group (n = 6). KYP-2047 (1 mg/ml) in saline containing 0.5% DMSO was injected

intraperitoneally (i.p., 3 mg/kg) twice a day (12/12 h) for 5 days. The vehicle group received the same treatment but with omission of KYP-2047 (same volume of 0.5% DMSO in saline). After 5 days of injections, the animals were sacrificed and tissues were removed as described above.

**Immunohistochemistry (IHC)**

IHC for the detection of α-syn in the mouse brain was performed by modifying the protocol described in Myöhänen *et al.,* (2010b). Briefly, the endogenous peroxidase activity was inactivated with 10% methanol and 3% $H_2O_2$ in Tris-buffered saline (TBS; pH 7.4) for 10 min, and non-specific binding was blocked with MOM Basic kit (Product BMK-2202, Vector laboratories, Burlingame, CA, USA) in TBS. The sections were incubated overnight at room temperature with α-syn antibody (Table 1), followed by washing with PBS. The slides were then incubated with goat anti-mouse HRP conjugated secondary antibody (Product #31430, Thermo Fisher Scientific; dilution 1:500 in TBS). The brown colour was developed with 0.05% 3,3'-diaminobenzidine and 0.03% hydrogen peroxide in TBS. Finally, the sections were transferred to objective glasses, dehydrated in alcohol series and mounted with Depex (BDH, Poole, UK). Slides were photographed and processed as described above.

In double-label immunofluorescence of PREP and α-syn, the protocol described in Myöhänen *et al.,* (2008a) was used. Briefly, free-floating sections were washed with PBS, and thereafter the double-label staining was carried out similarly as cells (see above).

**Semiquantitative analysis of optical density**

Immunohistochemically processed sections were photographed and the optical densities (OD) of the striatum, primary motor cortex and substantia nigra were analyzed using the line analysis tool of AnalySISpro software (version 5.0, Olympus Soft Imaging Solutions GmBH) as described in Lindholm *et al.* (2007). The background values of each brain area (background obtained by control

staining without primary antibody) were subtracted from raw data values of the same brain area. Altogether 15-20 samples of each brain area/staining from 3 different experiments were analyzed, and then the average and SEM of the values were calculated. OD-values of the WB images were analysed using the free-hand tool of QuantityOne-software (version 4.6.9, Bio-Rad) as described earlier (Myöhänen *et al.,* 2007). The bands in WB were quantified taking into account the OD (intensity) and the area of the band. When measuring the SDS-insoluble fractions of α-syn WB, the value of non-stressed wild-type cells was used as background that was subtracted from the value. In other WB analysis, after subtracting the background of the gel, the OD values were proportioned to the values of the loading control, and this value was considered indicative of the protein amounts. The averages and SEM of optical densities from each area were calculated.

**Statistical analysis**

Statistical analyses were performed using GraphPad Prism (version 5.0, GraphPad Software, Inc., San Diego, CA, USA). To detect difference between the groups in α-syn immunofluorescence, thioflavin S staining and cellular PREP enzyme activities, two-way ANOVA with Bonferroni post-test was used. Differences in α-syn OD values from animal IHC experiments were calculated with two-way ANOVA and Bonferroni post-test. Two-tailed Student t-test was used to assess the differences in cellular and animal WB results. Statistically significant differences were considered at $P < 0.05$.

## RESULTS

### Cell culture studies: KYP-2047 reduces α-synuclein immunoreactivity and aggregation in cells exposed to oxidative stress

*α-syn immunofluorescence*: The aggregation of α-syn was induced by oxidative stress (Stress 3d) in three stable SH-SY5Y cell lines overexpressing human WT, mutated A30P or A53T α-syn. The oxidative stress treatment with or without vehicle increased the percentage of cells with clearly elevated immunoreactive α-syn from control level (12% (A30P cells) - 26 % (WT α-syn)) up to 38% (A30P cells) - 48% (WT α-syn) (Fig. 1A-C, J). Vehicle (0.001% DMSO) or KYP-2047 incubation alone did not affect the number of cells with α-syn immunoreactivity (Fig. 1J). KYP-2047 significantly reduced the number of cells with immunoreactive α-syn both when present together with the oxidative stress (Stress 3 days with KYP; $P<0.001$ in all cell lines; Fig. 1D-F, J) or when incubated for one day after the oxidative stress treatment (Stress 3 days + 1 day KYP; $P<0.001$ in all cell lines; Fig. S1A in supplementary material) when compared to vehicle (Stress 3d with veh; Fig. 1A-C, J) in all α-syn overexpressing cell lines. Only minor α-syn immunoreactivity was seen in non-stressed cells with the antibody used in this study (Fig. 1G-I).

The effect of increasing concentrations of KYP-2047 (1 nM - 100 μM) on α-syn immunoreactivity was studied during the Stress 3d treatment of A30P and A53T cells. 1 nM of KYP-2047 in the culture medium did not cause any significant change in the number of cells with high α-syn immunoreactivity (Fig. S1B in supplementary material). At higher KYP-2047 concentrations, the number of cells with α-syn immunoreactivity was significantly reduced compared to Stress 3d with vehicle group ($P<0.001$; Fig. S1B in supplementary material).

*Soluble and insoluble α-syn protein levels detected by WB:* WB experiments of soluble and insoluble fractions of α-syn were performed to correlate the results obtained from the immunocytochemical analysis of all experimental conditions. A30P cells were used as a reference

in WB experiments. Stress 3d treatment with vehicle reduced the levels of soluble α-syn, and the amount of SDS-soluble monomers, but increased the amount of high-molecular-weight SDS-insoluble oligomers (Fig. 2A-D). The increase was not significant compared to non-stressed overexpressing cells, and the overexpression of A30P[α-syn] itself gave rise to some high-molecular-weight SDS-insoluble oligomers (Fig. 2A, C). However, the oxidative stress changed the pattern of high-molecular-weight bands that were accentuated (Fig. 2A). This was also seen as changing in staining pattern of cell immunohistochemistry (Fig. 1). Importantly, KYP-2047 incubation during the stress significantly reduced the levels of high-molecular-weight SDS-insoluble α-syn oligomers when administered with the oxidative stress (Fig. 2A, C; $P<0.05$ compared to Stress 3d with vehicle). KYP-2047 incubation without the stress decreased slightly (not significantly) SDS-soluble monomers (Fig. 2) but had no effect on soluble α-syn levels (Fig. 2A-B, D). Moreover, oxidative stress itself clearly decreased the levels of SDS-soluble α-syn monomers and slightly the levels of soluble α-syn (Fig. 2A, B, D). In non-stressed and non-overexpressing WT cells, hardly any SDS-soluble monomers or high-molecular-weight SDS-insoluble oligomers were seen (Fig. 2A).

*Thioflavin S staining as a marker of α-syn aggregation:* The results obtained by immunohistochemistry and WB experiments were confirmed by the appearance of thioflavin S (a specific marker for β-sheet structures) positive cells in the same conditions (Fig. 3A-C). In all cell lines, Thioflavin S staining was also significantly reduced by addition of KYP-2047 (Fig. 3D-G), supporting the IHC and WB results.

*α-syn mRNA transcription levels:* To clarify whether oxidative stress or PREP inhibitor have an effect on α-syn mRNA levels and protein transcription, a quantitative rtPCR experiment was performed for A30P cells. No changes in α-syn mRNA levels were detected in any condition tested (Table 2).

*Colocalization of α-syn with PREP*: We investigated potential colocalization of a-syn with PREP in all α-syn overexpressing cells by double-label immunofluorescence and confocal microscopy. PREP and α-syn partially colocalized when α-syn aggregation was induced by the Stress 3d treatment with vehicle (Fig. 4A-C). However, after incubation with KYP-2047, the observed colocalization was lost (Fig. 4D-E). KYP-2047 treatment did not affect the localization or amount of immunoreactive PREP (Fig. S2B in supplementary material), although some colocalization may have been lost due to the reduced amount of high-molecular-weight SDS-insoluble oligomers and SDS-soluble monomers as detected by WB (Fig. 2A-C). However, there was also a decrease of the PREP protein amounts due the oxidative stress, but not due the KYP-2047 incubation (Fig. S2B in supplementary material). In non-stressed cells, only minor colocalization was seen (Fig. 2B and Fig. 4G-I; Table 3). Since 1) the levels of soluble α-syn and SDS-soluble monomers were higher in non-stressed than stressed cells (Fig. 2C), and we detected 2) increased amount of high-molecular-weight SDS-insoluble α-syn and 3) increased colocalization between PREP and α-syn due the oxidative stress (Fig. 4A-C), our interpretation is that PREP colocalizes with α-syn aggregates (Fig. 1 and 4). The colocalization percentage in Stress 3d with vehicle varied between 24 % (A53T) and 42 % (WT α-syn). After KYP-2047 treatment, the percentages were 18-22% (Table 3). The colocalization percentages correlated with the amount of cells with α-syn inclusions (Fig. 1 and 3).

*PREP enzyme activity*: There was no significant difference in the PREP enzyme activities between the A30P, A53T or WT α-syn overexpressing cells and normal SH-SY5Y cells (Fig. S2A in supplementary material). 1 μM KYP-2047 drastically reduced the PREP activity in the cells during exposure to Stress 3d (Fig. S2A in supplementary material). The oxidative agents used slightly reduced PREP activity but this reduction was not statistically significant (Fig. S2A in supplementary material). This minor inhibition may be due to the fact that residual $Fe^{2+}$ ions from the culture medium inhibit PREP (Cunningham and O'Connor 1998).

*Cell viability*: To detect the effect of oxidative stress and PREP inhibition on cell viability of the A30P and A53T overexpressing cell lines and wild-type cells, standard LDH release assay was used. Moreover, to study the effect of oxidative stress on cell viability, we induced the aggregation of α-syn using 50%, 75% and 100% concentrations of oxidative stress medium. In the LDH cell viability assay, measuring the membrane integrity of the cells, KYP-2047 treatment reduced cell death in α-syn overexpressing cell lines compared to vehicle in all stress groups (Fig. 5A-C). The most significant differences were seen at 50% stress medium, but there was a significant difference also in 100% group (A53T cells; Fig. 5B). In non-overexpressing WT cells, the difference between vehicle and KYP-2047 was not visible (Fig. 5C), suggesting that the protective effect of KYP-2047 is related to α-syn overexpression. In 3-day KYP or vehicle incubations without oxidative stress, no clear differences in cell viability were observed (Fig. S3 in supplementary material).

**Animal studies: The effects of KYP-2047 in the brain of A30P α-syn transgenic mice**

*α-syn IHC and WB*: To confirm the *in vitro* and cellular effects of KYP-2047 on α-syn aggregation, we tested the effect of a 5-day treatment on the amount of α-syn immunoreactive and soluble protein levels in the brain of old Thy1-A30P-α-syn transgenic mice (Freichel *et al.,* 2007). Even this short exposure of KYP-2047 (3 mg/kg i.p. twice a day) significantly reduced the amount of α-syn protein in the A30P α-syn mice in all the brain areas analyzed (IHC), and in the whole-brain homogenates (WB) compared to vehicle treatment (Fig. 6A-M; Fig. S6A-B in supplementary material; WB, $P<0.01$ (mouse and human α-syn) and $P<0.05$ (human α-syn); IHC, $0.05<P<0.001$). Antibodies recognizing both human and mouse α-syn or only human α-syn showed similar effect (Fig. 6J-M), but the effect of the latter was more pronounced in the IHC analysis (Fig. 6K and 6M).

We also tested if the effect of KYP-2047 on the amount of the α-syn immunoreactivity/protein is dependent on the specific type of the α-syn mouse model, and performed the same experiment with a different A30P transgenic mouse strain where A30P α-syn is under the control of a prion promoter

(see details in Supplementary material and Yavich *et al.,* (2005)). The results in both mice strains were similar; a 5-day exposure of KYP-2047 (3 mg/kg) reduced the amount of α-syn to the levels found in the substantia nigra, striatum and motor cortex of the WT animals when analyzed with IHC (see details and Fig. S4 in supplementary material).

*Colocalization of PREP with αsyn:* Similar to the results of cellular studies, colocalization between α-syn and PREP was seen in the vehicle-treated transgenic mouse striatum (Fig. 7A) and substantia nigra pars compacta (Fig. 7C). After a 5-day KYP-2047 treatment, the colocalization clearly reduced (Fig. 7B and D), pointing to the ability of the PREP inhibitor to interfere with the interaction between α-syn and PREP also *in vivo*. However, some colocalization may have lost due to the reduced α-syn protein levels (Fig. 6A-M). Practically no colocalization was seen in the substantia nigra of a wild-type animal (Fig. 7E).

*PREP protein levels and PREP activity:* A 5-day KYP-2047 treatment (3 mg/kg i.p., twice a day) did not alter the amount of PREP protein amount assayed by WB in whole brains of A30P transgenic mouse (Fig. S5A in supplementary material). Moreover, KYP-2047 treatment did not significantly reduce the overall protein amounts in brain assayed by beta-actin WB of whole brain homogenate (Fig. S5B in supplementary material). There were also no statistical differences in PREP activity between A30P transgenic and WT mice measured from various brain areas (Fig. S5C in supplementary material).

## DISCUSSION AND CONCLUSIONS

To our knowledge, and based on this study it is the first time that a PREP inhibitor, KYP-2047, has been shown to reduce α-syn aggregation in cellular and animal models of Parkinson's disease. In the A30P α-syn overexpressing cells in culture, the PREP inhibitor reduced high-molecular-weight SDS-insoluble forms of α-syn induced by oxidative stress. In the A30P transgenic mouse

models, this reduction was also accompanied by a decrease in the amount of soluble α-syn in the brain.

Studies with cells in culture suggest that, when the α-syn aggregation process has been triggered by oxidative stress, the active site of PREP needs to be free to promote the aggregation, although PREP does not act as a trigger itself - this would cause a drop in the baseline of cells with overexpression upon inhibitor treatment. We have shown reliably that, under oxidative stress, a 3-day KYP-2047 incubation can reduce the amount of α-syn immunoreactivity and high-molecular-weight SDS-insoluble α-syn protein levels in α-syn overexpressing cells. Moreover, KYP-2047 treatment reduced β-sheet structure-containing cells revealed by Thioflavin S staining, pointing that KYP-2047 affects also α-syn aggregates. At least in the cell cultures, the reduction of α-syn level is not the result of the changes in transcription, and in α-syn overexpressing cells, PREP inhibition seems also to accelerate recovery of cells exposed to oxidative stress. Importantly, KYP-2047 also reduced the toxicity of oxidative stress on α-syn overexpressing cells assayed by the LDH cell viability assay. This was not observed in non-overexpressing cells, suggesting that KYP-2047 reduced the α-syn based cell toxicity. Similarly to cells, a 5-day treatment with KYP-2047 significantly reduced in α-syn immunoreactivity and soluble protein levels *in vivo*.

It was shown both in cells and *in vivo* that these proteins were partially colocalized when aggregation had occurred, and the colocalization was abolished by the PREP inhibitor. The reduced colocalization may also be caused by the decreased amount of α-syn or PREP proteins, especially in the mouse brain. However, in the cellular experiments, although the oxidative stress reduced also the amount of PREP protein, KYP-2047 did not have an additional effect. Moreover, at least in cells, the reduction in colocalization was more pronounced than the reduction of high-molecular-weight SDS-insoluble α-syn protein detected by WB. Therefore, it seems probable that colocalization disappears due to the effect of KYP-2047 rather than owing to the reduction in protein amounts. Moreover, in the non-stressed control cells only minor colocalization of PREP and

α-syn was seen, and oxidative stress even reduced the amounts of soluble α-syn and SDS-soluble monomers of α-syn below the non-stressed cells. This further supports the hypothesis that the interaction of PREP and α-syn occurs only after oxidative stress has triggered the aggregation process, and PREP colocalizes with aggregated forms of α-syn. These results support previous *in vitro* observations by Brandt et al. (2008) where, under cell-free conditions, the α-syn aggregation was accelerated by PREP, an effect that was blocked by two different PREP inhibitors (Z-pro-prolinal and UAMC-21) or by mutation of the active site of PREP.

There are several phases in the α-syn aggregation process. It has been suggested earlier, based on cell-free *in vitro* experiments, that PREP acts in early phases of α-syn aggregation, possibly in the nucleation phase (Lambeir 2011) but the mechanism remained unknown. It may be proposed that PREP acts as a nucleation center, and therefore assists the aggregation process. Moreover, we hypothesize that when KYP-2047 binds to PREP, the aggregation process is slowed down, giving time for cellular housekeeping mechanisms, such as proteasomes and lysosomes (Chu *et al.,* 2009; Lorenc-Koci *et al.,* 2011), to clear α-syn from the cells under the critical concentrations for aggregation (Wood *et al.,* 1999).

Since a PREP inhibitor accelerated the clearance of α-syn from the cells after the oxidative stress, and had potent effect on α-syn protein levels in old transgenic mouse, there are very probably some other mechanisms for PREP in α-syn aggregation process besides acting as a nucleation center. One possibility is that the PREP interaction with α-syn can interfere with the functions of aggresomes that are known to be the most effective in cleaning the α-syn aggregates (Opazo *et al*., 2008). PREP inhibition could then abolish the interaction and thus increase the activity of aggresomes. Aggresomal processing of misfolding proteins is also a microtubule-dependent process, and localization of PREP along the microtubules supports this function (Schulz *et al.,* 2005). The effect of KYP-2047 on a number of stressed α-syn overexpressing cells, that is seen in

immunohistochemistry, is very similar to aggresomal clearance reported earlier (Opazo *et al.,* 2008).

Eventually, the action of the PREP inhibitor leads also to a reduced number of aggregates, as shown by both WB and thioflavin S staining. PREP might also directly regulate the levels of α-syn protein by regulating gene expression, since recently Moreno-Baylach et al. (2011) reported that PREP and PREP inhibition can affect gene expression of various intracellular proteins. However, we did not see any changes in α-syn mRNA levels after PREP inhibition. According to our results, it is obvious that the active site or a specific active conformation of PREP is needed for the meaningful interaction of the two proteins. Further protein-protein interaction studies are obviously warranted.

Summarizing we conclude the following: 1) An incubation with KYP-2047 reduces the amount of high-molecular-weight SDS-insoluble α-syn oligomers in the α-syn overexpressing cells, and increases cell survival in the LDH assay. 2) Even a short-term treatment with KYP-2047 reduces the soluble α-syn *in vivo*. 3) PREP inhibitors are able to break the spatial interaction between PREP and α-syn in three different α-syn overexpressing cell lines and also *in vivo*. This is proposed to lead to a block of the α-syn aggregation process or to an enhancement of the α-syn clearance. Although these findings suggest that PREP may increase the α-syn aggregation via protein-protein interaction, the molecular mechanism remains unclear. The fast and significant effect of a short-term exposure to a PREP inhibitor on levels of α-syn and its aggregation may open new ways to develop a drug therapy for α-syn based Parkinson's disease.

**ACKNOWLEDGEMENTS**

The authors thank the Department of Veterinary Sciences and the Core Facility Biomedical Microscopic Imaging of the University of Antwerp for providing excellent facilities for tissue

processing and staining, Prof. P.P. De Deyn, Dr D. Van Dam and members of the Laboratory of Neurochemistry and Behaviour of the University of Antwerp for housing mice and their assistance studying mice behaviour, and Dr. P. Jäkälä (University of Eastern Finland) and Dr. P. Kahle (University of Tübingen) for providing the A30P transgenic mice. We also acknowledge M.Sc. G. Duran-Torres for his excellent technical assistance. These studies were supported by grants from FWO-Vlaanderen, UA Research Council, Finnish Cultural Foundation, Orion-Pharmos Foundation, Academy of Finland (No. 138127/2010) and Jane and Aatos Erkko Foundation to Timo T. Myöhänen, by the grants of the Academy of Finland (No. 1131915/2008 and No. 117881/2006) to Pekka T. Männistö, and by the grant (G.0114.08) of the FWO-Vlaanderen to Anne-Marie Lambeir and Veerle Baekelandt. This research was supported by the nEuroPro project, EU FP7-HEALTH-2007-B- 223077.

**REFERENCES**

Alexander, SPH, Mathie, A, Peters, JA (2009). Guide to Receptors and Channels (GRAC), 4th edition. *Br J Pharmacol* 158 (Suppl. 1): S1–S254.

Arima K, Ueda K, Sunohara N, Hirai S, Izumiyama Y, Tonozuka-Uehara H *et al*. (1998). Immunoelectron-microscopic demonstration of NACP/alpha-synuclein-epitopes on the filamentous component of Lewy bodies in Parkinson's disease and in dementia with Lewy bodies. *Brain Res* 808: 93-100.

Bisaglia M, Mammi S, Bubacco L. (2009). Structural insights on physiological functions and pathological effects of alpha-synuclein. *FASEB J* 23: 329-340.

Bradford MM. (1976). A rapid and sensitive method for the quantitation of microgram quantities of protein utilizing the principle of protein-dye binding. *Anal Biochem* 72 248-254.

Brandt I, Gerard M, Sergeant K, Devreese B, Baekelandt V, Augustyns K *et al*. (2008). Prolyl oligopeptidase stimulates the aggregation of alpha-synuclein. *Peptides* 29: 1472-1478.

Chu Y, Dodiya H, Aebischer P, Olanow CW, Kordower JH. (2009). Alterations in lysosomal and proteasomal markers in Parkinson's disease: relationship to alpha-synuclein inclusions. *Neurobiol Dis* 35: 385-398.

Conway KA, Harper JT, Landsbury PT Jr. (2000). Fibrils formed in vitro from alpha-synuclein and two mutant forms linked to Parkinson's disease are typical amyloid. *Biochemistry* 39*:* 2552-2563.

Cooper AA, Gitler AD, Cashikar A, Haynes CM, Hill KJ, Bhullar B *et al*. (2006). Alpha-synuclein blocks ER-Golgi traffic and Rab1 rescues neuron loss in Parkinson's models. *Science* 313: 324-328.

Cunningham DF, O'Connor B (1998). A study of prolyl endopeptidase in bovine serum and its relevance to the tissue enzyme. *Int J Biochem Cell Biol* 30: 99-114.

Deleersnijder A, Van Rompuy AS, Desender L, Pottel H, Buee L, Debyser Z *et al*. (2011). Comparative analysis of different peptidyl-prolyl isomerases reveals FK506-binding protein 12 as the most potent enhancer of {alpha}-synuclein aggregation. *J Biol Chem*

Di Daniel E, Glover CP, Grot E, Chan MK, Sanderson TH, White JH *et al*. (2009). Prolyl oligopeptidase binds to GAP-43 and functions without its peptidase activity. *Mol Cell Neurosc* 41:373-382.

Feng LR, Federoff HJ, Vicini S, Maguire-Zeiss KA. (2010). α-Synuclein mediates alterations in membrane conductance: a potential role for α-synuclein oligomers in cell vulnerability. *Eur J Neurosci* 32: 10-17.

Freichel C, Neumann M, Ballard T, Muller V, Woolley M, Ozmen L *et al*. (2007). Age-dependent cognitive decline and amygdala pathology in alpha-synuclein transgenic mice. *Neurobiol Aging* 28: 1421-1435.

Garcia-Horsman JA, Männistö PT, Venäläinen JI. (2007). On the role of prolyl oligopeptidase in health and disease. *Neuropeptides* 41: 1-24.

Gerard M, Debyser Z, Desender L, Baert J, Brandt I, Baekelandt V *et al*. (2008). FK506 binding protein 12 differentially accelerates fibril formation of wild type alpha-synuclein and its clinical mutants A30P or A53T. *J Neurochem* 106: 121-133.

Gerard M, Deleersnijder A, Daniels V, Schreurs S, Munck S, Reumers V *et al.* (2010). Inhibition of FK506 binding proteins reduces alpha-synuclein aggregation and Parkinson's disease-like pathology. *J Neurosci* 30: 2454-2463.

Ibanez P, Bonnet AM, Debarges B, Lohmann E, Tison F, Pollak P *et al.* (2004). Causal relation between alpha-synuclein gene duplication and familial Parkinson's disease. *Lancet* 364: 1169-1171.

Jalkanen AJ, Puttonen KA, Venäläinen JI, Sinervä V, Mannila A, Ruotsalainen S *et al*. (2007). Beneficial effect of prolyl oligopeptidase inhibition on spatial memory in young but not in old scopolamine-treated rats. *Basic Clin Pharmacol Toxicol* 100: 132-138.

Jalkanen AJ, Hakkarainen JJ, Lehtonen M, Venäläinen T, Kääriäinen TM, Jarho E *et al.* (2011). Brain pharmacokinetics of two prolyl oligopeptidase inhibitors, JTP-4819 and KYP-2047, in the rat. *Basic Clin Pharmacol Toxicol* doi: 10.1111/j.1742-7843.2011.00747.x

Jarho EM, Venäläinen JI, Huuskonen J, Christiaans JA, Garcia-Horsman JA, Forsberg MM, Jarvinen T *et al*. (2004). A cyclopent-2-enecarbonyl group mimics proline at the P2 position of prolyl oligopeptidase inhibitors. *J Med Chem* 47: 5605-5607.

Kahle PJ, Neumann M, Ozmen L, Muller V, Jacobsen H, Schindzielorz A *et al.* (2000). Subcellular localization of wild-type and Parkinson's disease-associated mutant alpha -synuclein in human and transgenic mouse brain. *J Neurosci* 20: 6365-6373.

Kato A, Fukunari A, Sakai Y, Nakajima T. (1997). Prevention of amyloid-like deposition by a selective prolyl endopeptidase inhibitor, Y-29794, in senescence-accelerated mouse. *J Pharmacol Exp Ther* 283: 328-335.

Kim M, Jung W, Lee IH, Bhak G, Paik SR, Hahn JS. (2008). Impairment of microtubule system increases alpha-synuclein aggregation and toxicity. *Biochem Biophys Res Commun* 365: 628-635.

Kruger R, Kuhn W, Muller T, Woitalla D, Graeber M, Kosel S *et al.* (1998). Ala30Pro mutation in the gene encoding alpha-synuclein in Parkinson's disease. *Nat Genet* 18: 106-108.

Lambeir AM. (2011). Interaction of Prolyl Oligopeptidase with -Synuclein. *CNS Neurol Disord Drug Targets* 10: 349-354.

Lindholm P, Voutilainen MH, Lauren J, Peränen J, Leppänen VM, Andressoo JO *et al.* (2007). Novel neurotrophic factor CDNF protects and rescues midbrain dopamine neurons in vivo. *Nature* 448: 73-77.

Lorenc-Koci E, Lenda T, Antkiewicz-Michaluk L, Wardas J, Domin H, Smialowska M *et al.* (2011). Different effects of intranigral and intrastriatal administration of the proteasome inhibitor lactacystin on typical neurochemical and histological markers of Parkinson's disease in rats. *Neurochem Int*

Männistö PT, Venäläinen JI, Jalkanen AJ, Garcia-Horsman JA. (2007). Prolyl oligopeptidase: A potential target for the treatment of cognitive disorders. *Drugs News Persp* 20: 293-305.

Mantle D, Falkous G, Ishiura S, Blanchard PJ, Perry EK. (1996). Comparison of proline endopeptidase activity in brain tissue from normal cases and cases with Alzheimer's disease, Lewy body dementia, Parkinson's disease and Huntington's disease. *Clin Chim Acta* 249: 129-139.

McLean PJ, Kawamata H, Ribich S, Hyman BT. (2000). Membrane association and protein conformation of alpha-synuclein in intact neurons. Effect of Parkinson's disease-linked mutations. *J Biol Chem* 275: 8812-8816.

Moreno-Baylach MJ, Felipo V, Männistö PT, Garcia-Horsman JA. (2008). Expression and traffic of cellular prolyl oligopeptidase are regulated during cerebellar granule cell differentiation, maturation, and aging. *Neuroscience* 156: 580-585.

Moreno-Baylach MJ, Puttonen KA, Tenorio-Laranga J, Venäläinen JI, Storvik M, Forsberg MM *et al*. (2011). Prolyl Endopeptidase Is Involved in Cellular Signalling in Human Neuroblastoma SH-SY5Y Cells. *Neurosignals* 19: 97-109.

Myöhänen TT, Schendzielorz N, Männistö PT. (2010a). Distribution of catechol-O-methyltransferase (COMT) proteins and enzymatic activities in wild-type and S-COMT deficient mice. *J Neurochem* 113: 1632-43

Myöhänen T, Tenorio-Laranga J, Jokinen B, Vazquez-Sanchez R, Moreno-Baylach M, Garcia-Horsman J *et al.* (2010b). Prolyl oligopeptidase induces angiogenesis both in vitro and in vivo in a novel regulatory manner. *Br J Pharmacol* 163: 1666-1678

Myöhänen TT, Venäläinen JI, Tupala E, Garcia-Horsman JA, Miettinen R, Männistö PT. (2007). Distribution of Immunoreactive Prolyl Oligopeptidase in Human and Rat Brain. *Neurochem Res* 32: 1365-1374.

Myöhänen TT, Venäläinen JI, Garcia-Horsman JA, Piltonen M, Männistö PT. (2008a). Cellular and subcellular distribution of rat brain prolyl oligopeptidase and its association with specific neuronal neurotransmitters. *J Comp Neurol* 507: 1694-1708.

Myöhänen TT, Venäläinen JI, Garcia-Horsman JA, Piltonen M, Männistö PT. (2008b). Distribution of prolyl oligopeptidase in the mouse whole-body sections and peripheral tissues. *Histochem Cell Biol* 130: 993-1003.

Neumann M, Kahle PJ, Giasson BI, Ozmen L, Borroni E, Spooren W *et al*. (2002). Misfolded proteinase K-resistant hyperphosphorylated alpha-synuclein in aged transgenic mice with locomotor deterioration and in human alpha-synucleinopathies. *J Clin Invest* 110: 1429-1439.

Opazo F, Krenz A, Heermann S, Schulz JB, Falkenburger BJ. (2008). Accumulation and clearance of α-synuclein aggregates demonstrated by time-lapse imaging. *J Neurochem* 106: 529-540.

Polymeropoulos MH, Lavedan C, Leroy E, Ide SE, Dehejia A, Dutra A *et al.* (1997). Mutation in the alpha-synuclein gene identified in families with Parkinson's disease. *Science* 276: 2045-2047.

Shishido Y, Furushiro M, Tanabe S, Taniguchi A, Hashimoto S, Yokokura T *et al.* (1998). Effect of ZTTA, a prolyl endopeptidase inhibitor, on memory impairment in a passive avoidance test of rats with basal forebrain lesions. *Pharm Res* 15: 1907-1910.

Singleton AB, Farrer M, Johnson J, Singleton A, Hague S, Kachergus J *et al.* (2003). alpha-synuclein locus triplication causes Parkinson's disease. *Science* 302: 841

Singleton A, Gwinn-Hardy K, Sharabi Y, Li ST, Holmes C, Dendi R *et al.* (2004). Association between cardiac denervation and parkinsonism caused by alpha-synuclein gene triplication. *Brain* 127: 768-772

Spillantini MG, Schmidt ML, Lee VM, Trojanowski JQ, Jakes R, Goedert M. (1997). Alpha-synuclein in Lewy bodies. *Nature* 388: 839-840.

Surguchov A. (2008). Molecular and cellular biology of synucleins. *Int Rev Cell Mol Biol* 270: 225-317.

Talman V, Tuominen RK, Boije af Gennäs G, Yli-Kauhaluoma J, Ekokoski E. (2011) C1 Domain-targeted isophthalate derivatives induce cell elongation and cell cycle arrest in HeLa cells. *PLoS One* 6: e20053.

Toide K, Shinoda M, Fujiwara T, Iwamoto Y. (1997). Effect of a novel prolyl endopeptidase inhibitor, JTP-4819, on spatial memory and central cholinergic neurons in aged rats. *Pharmacol Biochem Behav* 56: 427-434.

Uversky VN, Li J, Fink AL. (2001). Evidence for a partially folded intermediate in alpha-synuclein fibril formation. *J Biol Chem* 276: 10737-10744.

Venäläinen JI, Garcia-Horsman JA, Forsberg MM, Jalkanen A, Wallen EA, Jarho EM *et al*. (2006). Binding kinetics and duration of in vivo action of novel prolyl oligopeptidase inhibitors. *Biochem Pharmacol* 71: 683-692.

Wood SJ, Wypych J, Steavenson S, Louis JC, Citron M, Biere AL. (1999). alpha-synuclein fibrillogenesis is nucleation-dependent. Implications for the pathogenesis of Parkinson's disease. *J Biol Chem* 274: 19509-19512.

Yavich L, Oksman M, Tanila H, Kerokoski P, Hiltunen M, van Groen T *et al.* (2005). Locomotor activity and evoked dopamine release are reduced in mice overexpressing A30P-mutated human alpha-synuclein. *Neurobiol Dis* 20: 303-313.

Yoshimoto T, Kado K, Matsubara F, Koriyama N, Kaneto H, Tsura D. (1987). Specific inhibitors for prolyl endopeptidase and their anti-amnesic effect. *J Pharmacobiodyn* 10: 730-735.

Yu S, Li X, Liu G, Han J, Zhang C, Li Y *et al.* (2007). Extensive nuclear localization of alpha-synuclein in normal rat brain neurons revealed by a novel monoclonal antibody. *Neuroscience* 145: 539-555.

Zarranz JJ, Alegre J, Gomez-Esteban JC, Lezcano E, Ros R, Ampuero I *et al.* (2004). The new mutation, E46K, of alpha-synuclein causes Parkinson and Lewy body dementia. *Ann Neurol* 55: 164-173.

**Table 1.** Details of Primary Antibodies

| **Antigen** | **PREP** | **Human α-syn** | **Human and mouse α-syn** | **β-actin** |
|---|---|---|---|---|
| **Marker for** | PREP protein | Human α-syn protein | Human and mouse α-syn protein | Loading control (WB) |
| **Species** | Chicken IgY | Mouse monoclonal; clone 4B12 | Mouse monoclonal; clone 3H9 | Mouse monocolonal; clone AC-15 |
| **Immunogen** | Purified pig PREP | Whole-length recombinant human α-syn | Whole-length recombinant human α-syn | synthetic beta-cytoplasmic N-ternimal peptide |
| **Manufacturer** | Venäläinen et al. 2006 | AbCam, Cambridge, UK; Thermo Fisher Scientific, Waltham, MA, USA | AbCam, Cambridge, UK | Sigma-Aldrich |
| **Product #** | - | ab1904; MA1-90346 | ab78155 | A1978 |
| **Dilution used** | 1:500 (IHC)<br>1:5000 (WB) | 1:1000 (IFL)<br>1:600 (IHC)<br>1:10000 (WB) | 1:1000 (IHC)<br>1:2000 (WB in α-syn fractions)<br>1:10000 (WB) | 1:3000 (WB) |
| **Specificity and reference** | WB (human and mouse), (Myöhänen *et al.,* 2007; Myöhänen *et al.,* 2008b); | WB; AbCam and Thermo Fisher datasheets, our experiments | WB; AbCam datasheet, our experiments | WB; our experiments |

IFL, cell immunofluorescence; IHC, immunohistochemistry; WB, Western blot

**Table 2.** Transcription changes of α-syn gene, relative to the β-actin control gene, assayed by quantitative reverse transcriptase PCR in A30P overexpressing cells after 3-day oxidative stress and controls (value ± standard deviation (sd)).

| | $2^{-\Delta\Delta C(t)} \pm$ sd* |
|---|---|
| 3 d Stress with VEH | 1.33 ± 0.4 |
| 3 d Stress with 1 μM KYP-2047 | 1.37 ± 0.8 |
| 3 d 1 μM KYP-2047 | 1.13 ± 0.1 |
| Control | 1.33 ± 0.1 |

* Average of 3 measurements

**Table 3.** Colocalization percentages between PREP and α-synuclein in overexpressing cell lines (% of all cells ± SEM). All values are averages of 3 individual experiments.

| | A30P | A53T | WT α-syn |
|---|---|---|---|
| 3 d Stress with vehicle | 31 ± 1.6 | 24 ± 2.2 | 42 ± 3.8 |
| 3 d Stress with 1 μM KYP-2047 | 18 ± 2.3 ** | 11 ± 2.2 ** | 20 ± 1.7 *** |
| 3 d 1 μM KYP-2047 | 10 ± 0.3 | 12 ± 1.9 | 17 ± 2.2 |
| Control | 12 ± 2.1 | 11 ± 1.3 | 19 ± 1.3 |

**, $P<0.01$; ***, $P<0.001$ compared to 3d Stress with vehicle

## FIGURE LEGENDS

**Figure 1A-J. The effect of KYP-2047 on immunoreactive α-syn in three different α-syn overexpressing cell lines.** Representative confocal photomicrographs are depicting that oxidative stress of 3 days with vehicle (0.001% DMSO; Stress 3d with veh) clearly increased the amount of cells with highly immunoreactive α-syn in all cell lines as seen in panels A-C and J (α-syn is visualized with green, nuclear marker DAPI is visualized with blue). Incubation of 1 μM KYP-2047 during the oxidative stress (Panels D-G; Stress 3d with KYP) significantly reduced the cells with immunoreactive α-syn in all cell lines ($P<0.001$; Panel J), Incubation of cells with KYP-2047 without oxidative stress did not affect the α-syn immunoreactivity (Panel J, KYP 3d). In non-stressed control cells (Panels G-I, Control), only low amount of α-syn immunoreactivity was seen. Bars are Mean±SEM in G-H (n = 3 individual experiments). Scale bars are 10 μm in all the images. For detailed information of study groups, see materials and methods. ***, $P<0.001$ Stress 3d with veh vs. Stress 3d with KYP; Cell line codes: A30P cells, SH-SY5Y cells expressing human A30P mutated α-syn; A53T cells, SH-SY5Y cells expressing human A53T mutated α-syn; WT asyn cells, SH-SY5Y cells expressing human wild-type α-syn.

**Figure 2A-D. The effect of oxidative stress and KYP-2047 on SDS-insoluble α-syn on Western blot.** In non-stressed A30P control cells (A30P control) and in non-stressed A30P cells incubated with KYP-2047 (KYP 3d), some high-molecular-weight SDS-insoluble oligomers were seen due to their A30P[α-syn] overexpression (Panel A). In non-stressed and non-overexpressing WT cells (WT control; Panel A), hardly any SDS-soluble monomers or high-molecular-weight SDS-insoluble oligomers were seen. OD value of WT control was used as a background value in WB band OD analysis of A30P cells. A 3-day oxidative stress with vehicle (0.001% DMSO; Stress 3d with veh) increased the amount (not significantly compared to A30P control, $p = 0.094$) and changed the pattern of high-molecular-weight SDS-insoluble α-syn (black vertical bar; Panel A and C). Oxidative stress caused reduction of SDS-soluble monomers (black arrow, Panel A, B; $p<0.01$), and also some decrease in soluble α-syn (black arrowhead, Panel A and D). Incubation with KYP-2047 during stress reduced high-molecular-weight SDS-insoluble α-syn in WB compared to vehicle incubation ($p<0.05$, Student t-test; Stress 3d with veh vs. Stress 3d with KYP; black vertical bar; Panel A-B). Only slight reduction by KYP-2047 was seen in SDS-soluble α-syn monomers or soluble α-syn (black arrow and black arrowhead; Panel B, D). Representative α-syn Western blot bands are from A30P cells. For detailed information of study groups, see materials and methods. Bars are Mean±SEM in B-D (n = 3 independent experiments). *, $P<0.05$ in Stress 3d with veh vs. Stress 3d with KYP. **, $P<0.01$ in Stressed vs. non-stressed cells.

**Figure 3A-G. Thioflavin S staining of protein aggregates in three different α-syn overexpressing cells.** Thioflavin S stained fluorescence photomicrographs are very similar to the results of α-syn immunofluorescence in Fig. 1. Incubation of 1 μM KYP-2047 during the 3-day oxidative stress (Stress 3d with KYP; Panels D-F) reduced significantly the amount of cells with cytosolic aggregates compared to vehicle incubation (Stress 3d with veh; Panel A-C) in all cell lines (Panel G; $P<0.01$). Similar to immunofluorescence staining, treatment with

the PREP inhibitor without the oxidative stress did not cause any difference in aggregates compared to the control (G; KYP 3d). Bars are Mean±SEM in panel I (n = 3 individual experiments); **, P<0.01 Stress 3d with veh vs. Stress 3d with KYP. Cell line codes are similar to Fig. 1. Scale bars are 10 µm in all the images.

**Figure 4A-I. Changes in colocalization between PREP and α-syn during oxidative stress vehicle (Stress 3d with vehicle) and PREP inhibitor treatment (Stress 3d with KYP) visualized by IHC and confocal microscopy.** When α-syn overexpressing cells are exposed to Stress for 3 days with vehicle (Panels A-C), partial intracellular colocalization between α-syn (green) and PREP (magenta) is formed (white colour, white arrows). However, when 1 µM KYP-2047 is present (Stress 3d with KYP, Panels D-E), the colocalization disappears. Small picture panels in Panels A-E are magnifications from the larger picture, depicting the colocalization and its disappearance after KYP-2047 incubation. In non-stressed cells, only scarce colocalization between PREP and α-syn is seen (Control, Panels G-I). Cell line codes are as in Fig. 1. Scale bars are 10 µm in large images and 1 µm in small picture panels.

**Figure 5A-C. The effect of 3-day oxidative stress with vehicle or KYP-2047 on cell viability studied by lactate dehydrogenase (LDH) assay.** Cell viability was measured using different concentrations of oxidative stress medium (100%, 75% and 50%), and A30P (Panel A) and A53T (Panel B) cells. Wild-type (WT) cells (without α-syn overexpression) were used as a control (Panel C). In α-syn overexpressing cells, KYP-2047 (red line) clearly reduced the cell death compared to vehicle (green line), and the difference was significant even in 100% stress medium (A53T cells; Panel B). The most significant effects were seen in 50% stress medium (Panels A-B). In WT cells, no statistical differences were seen in any stress concentration (Panel C). n = 5 individual experiments. **, P<0.01 Stress 3d with veh vs. Stress 3d with KYP; *, P<0.05 Stress 3d with veh vs. Stress 3d with KYP; (*), P = 0.054 Stress 3d with veh vs. Stress 3d with KYP in A30P cells and 75% stress medium.

**Figure 6A-M. The effect of a 5-day KYP-2047 exposure on α-syn protein expression in A30P α-syn transgenic mice.** A clear effect of PREP inhibition (A30P KYP-2047) was seen on immunoreactive α-syn in various brain areas of A30P α-syn transgenic mice (Panels A-K; 0.05<P<0.001), and also in the whole-brain α-syn determined with Western blot (WB; Panels L-M; 0.05<P<0.01). The effect is accentuated in A30P mutated human α-syn by the IHC analysis (Panels J-K). Panels L-M are depicting α-syn detected by WB from KYP-2047 and vehicle (veh) exposed A30P α-syn transgenic mouse brain. Representative WB bands are presented in Fig. S6A-B in supplementary material. Bars are Mean±SEM in panels J-M (n = 3 individual experiments). Scale bars are 100 µm. *, P<0.05; **, P<0.01; ***, P<0.001 vs. A30P vehicle (A30P veh). Codes: A30P KYP-2047, PREP inhibitor treated A30P α-syn transgenic mouse; A30P veh, vehicle treated A30P α-syn transgenic mouse; M1, primary motor cortex; SN, substantia nigra; Stri, striatum; WT, wild-type animal.

**Figure 7A-E. Confocal immunofluorescence pictures presenting the *in vivo* colocalization between α-syn and PREP in nigrostriatal path.** Clear colocalization is seen both in striatum (panel A, Stri) and substantia nigra (panel C, SN) of vehicle (A30P veh) treated A30P α-syn transgenic mice while in KYP-2047 exposed animals the colocalization was not present (panels B, D). In the substantia nigra of wild-type (WT) mice very minor amounts of α-syn were seen (E). α-syn is visualized with fluorescein (green), PREP with Texas red (magenta) and nuclei with DAPI (blue). Pictures are merged and colocalization

between α-syn and PREP is shown in white color (white arrows). Scale bars are 10 μm in all figures. Codes are similar to Fig. 6.

The authors state that they have no conflicts of interests.

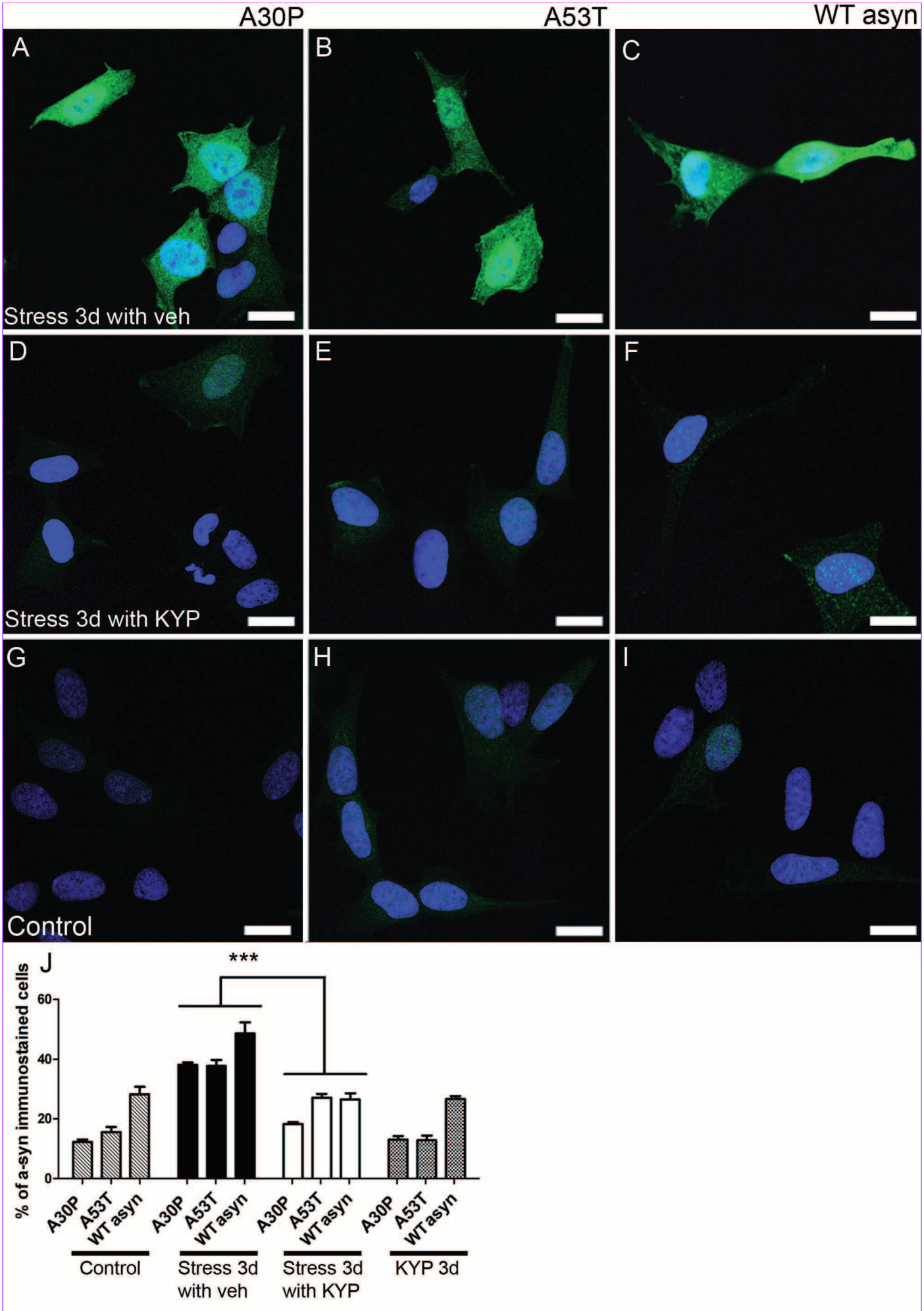
A30P
A53T
WT asyn
A
B
C
Stress 3d with veh
D
E
F
Stress 3d with KYP
G
H
I
Control
J
***
% of a-syn immunostained cells
60
40
20
0
A30P
A53T
WT asyn
Control
Stress 3d with veh
Stress 3d with KYP
KYP 3d

Fig1

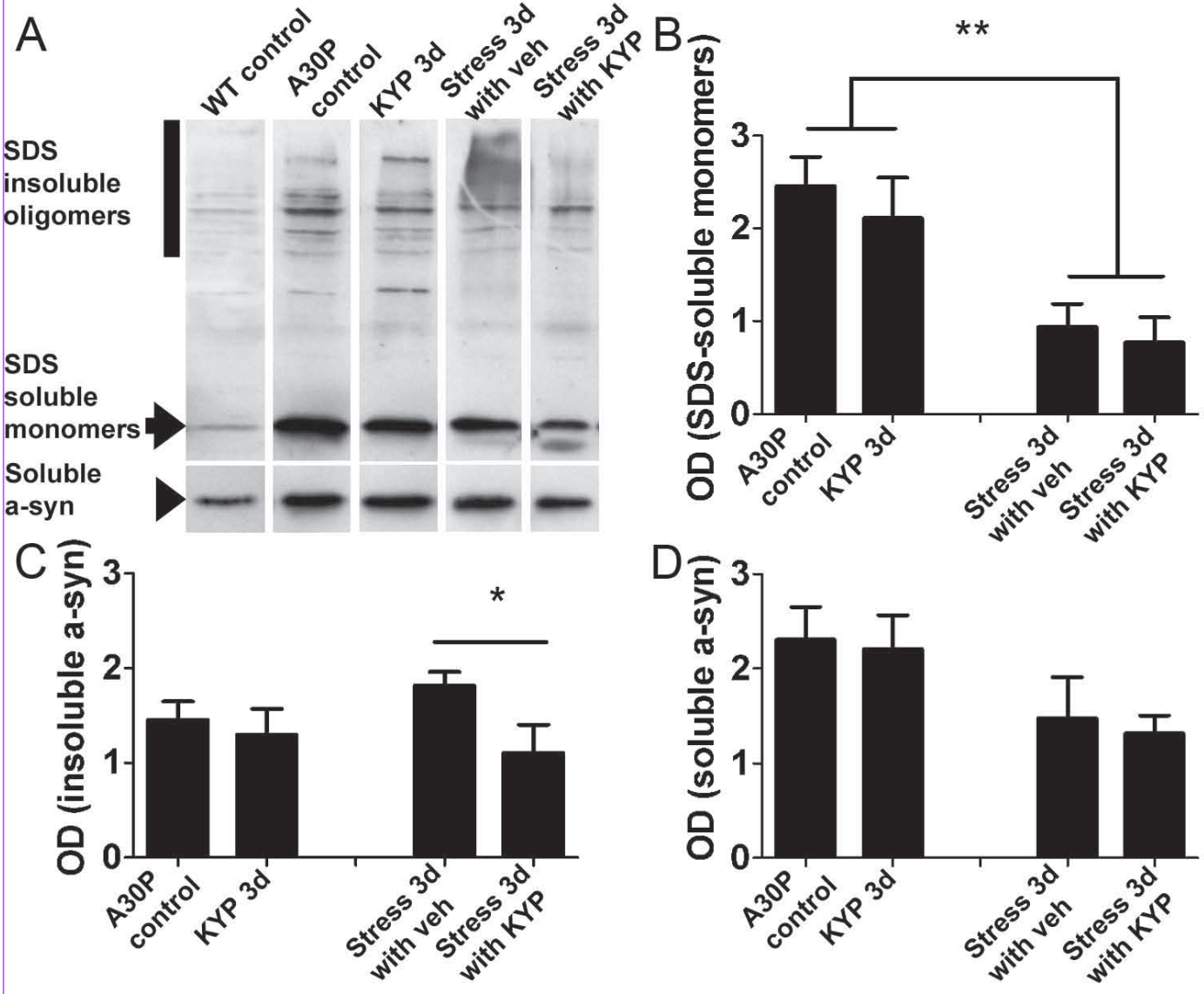
A
WT control
A30P control
KYP 3d
Stress 3d with veh
Stress 3d with KYP
SDS insoluble oligomers
SDS soluble monomers
Soluble a-syn
B
**
OD (SDS-soluble monomers)
A30P control
KYP 3d
Stress 3d with veh
Stress 3d with KYP
C
*
OD (insoluble a-syn)
D
OD (soluble a-syn)

Fig2

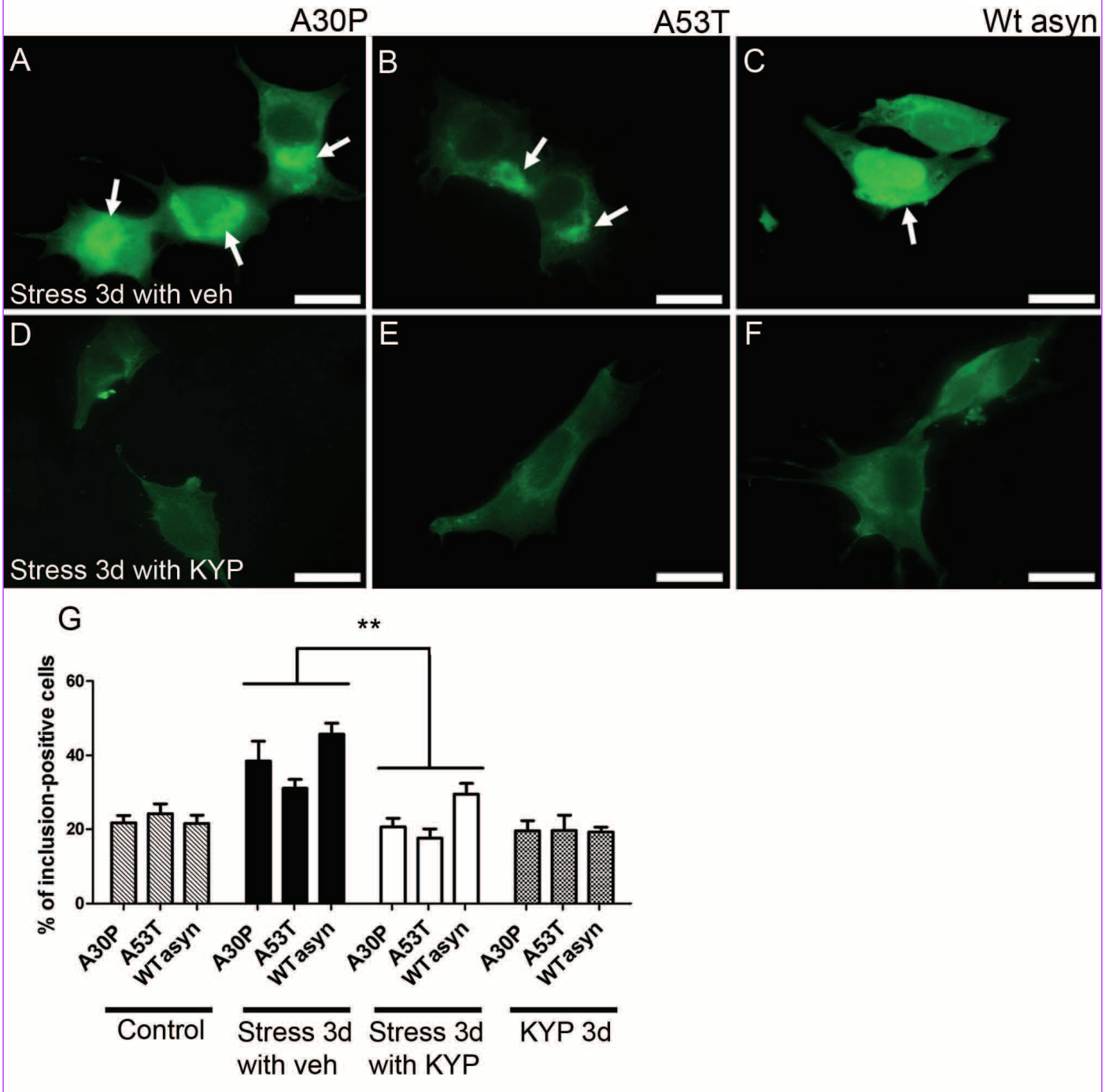
A30P
A53T
Wt asyn
A
B
C
Stress 3d with veh
D
E
F
Stress 3d with KYP
G
**
% of inclusion-positive cells
60
40
20
0
A30P
A53T
WTasyn
Control
Stress 3d with veh
Stress 3d with KYP
KYP 3d

Fig3

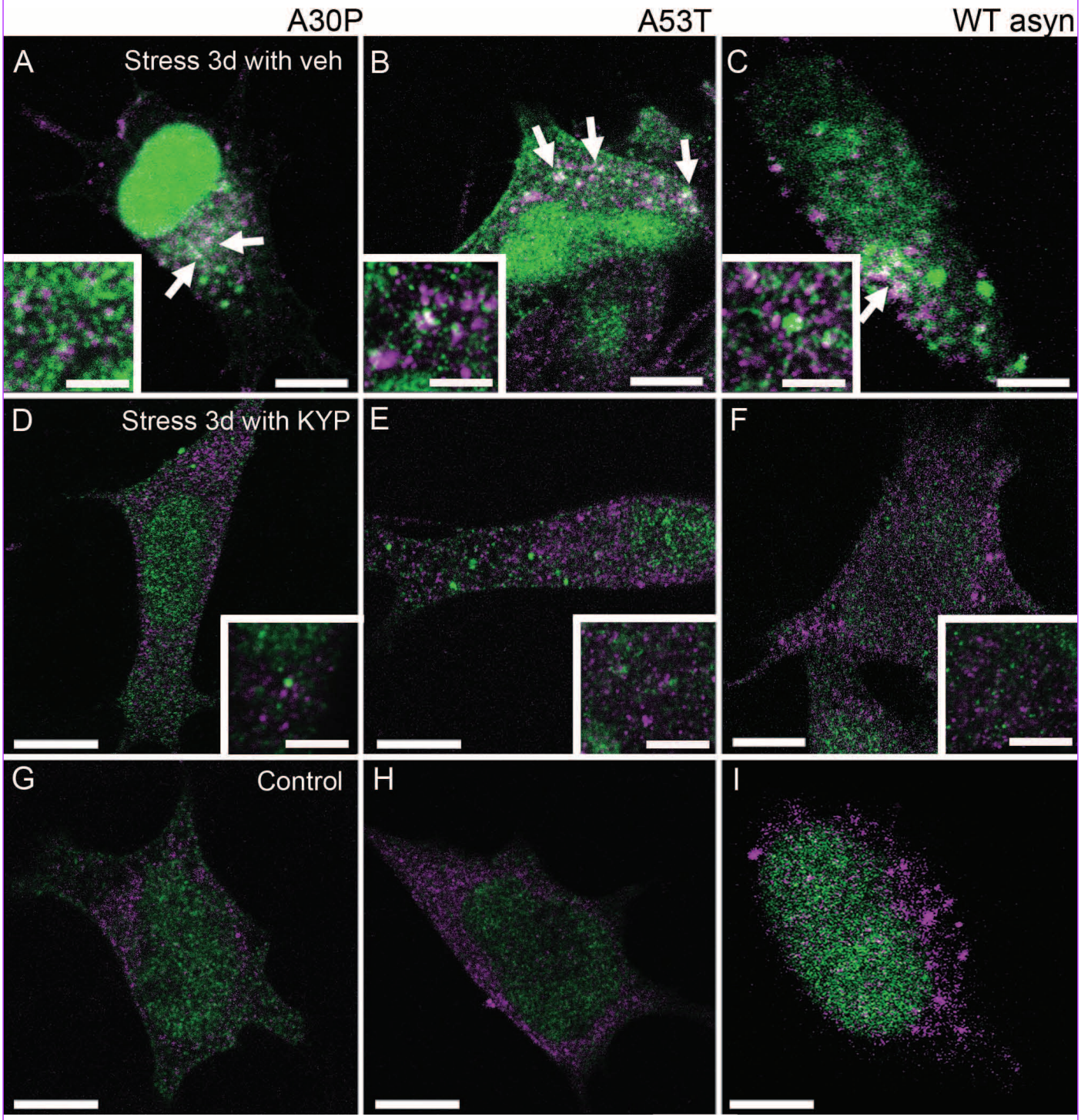
A30P
A53T
WT asyn
A
Stress 3d with veh
B
C
D
Stress 3d with KYP
E
F
G
Control
H
I

Fig4

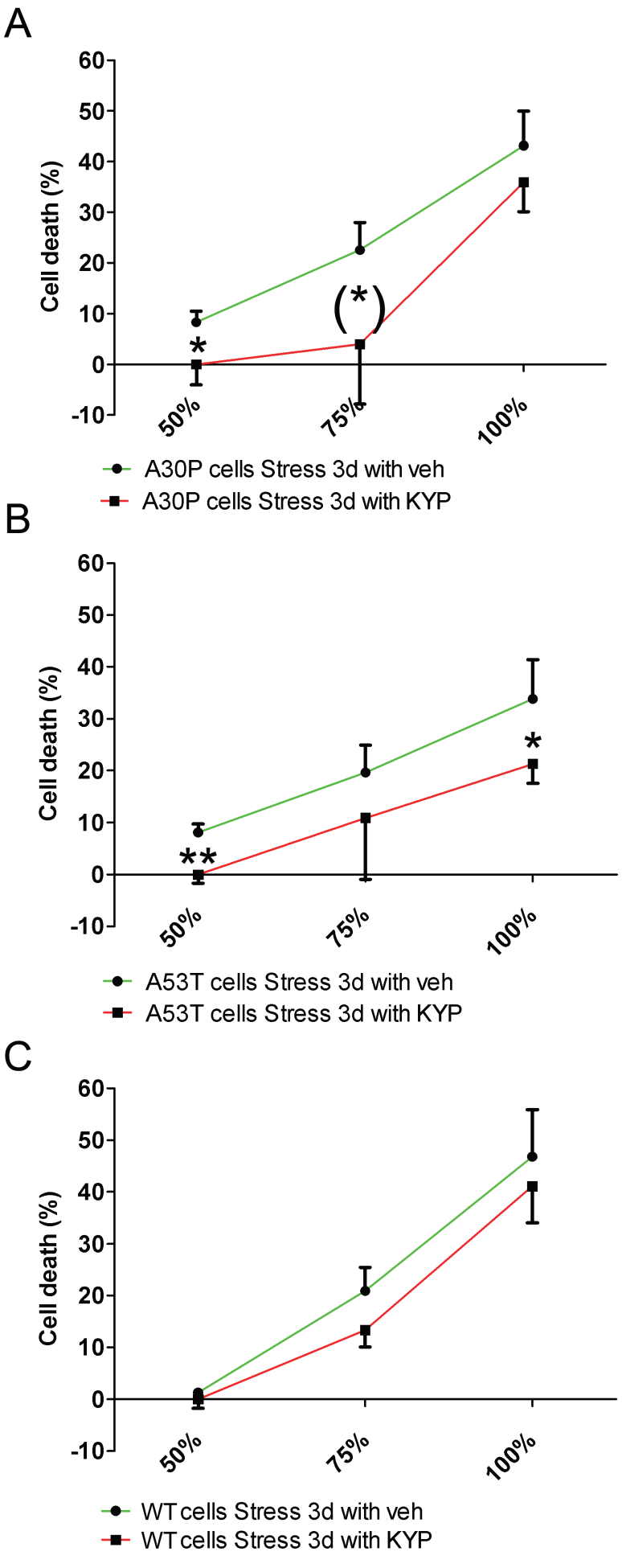
A
60
50
40
30
20
10
0
-10
Cell death (%)
(*)
*
50%
75%
100%
A30P cells Stress 3d with veh
A30P cells Stress 3d with KYP
B
60
50
40
30
20
10
0
-10
Cell death (%)
**
*
50%
75%
100%
A53T cells Stress 3d with veh
A53T cells Stress 3d with KYP
C
60
50
40
30
20
10
0
-10
Cell death (%)
50%
75%
100%
WT cells Stress 3d with veh
WT cells Stress 3d with KYP

Fig5

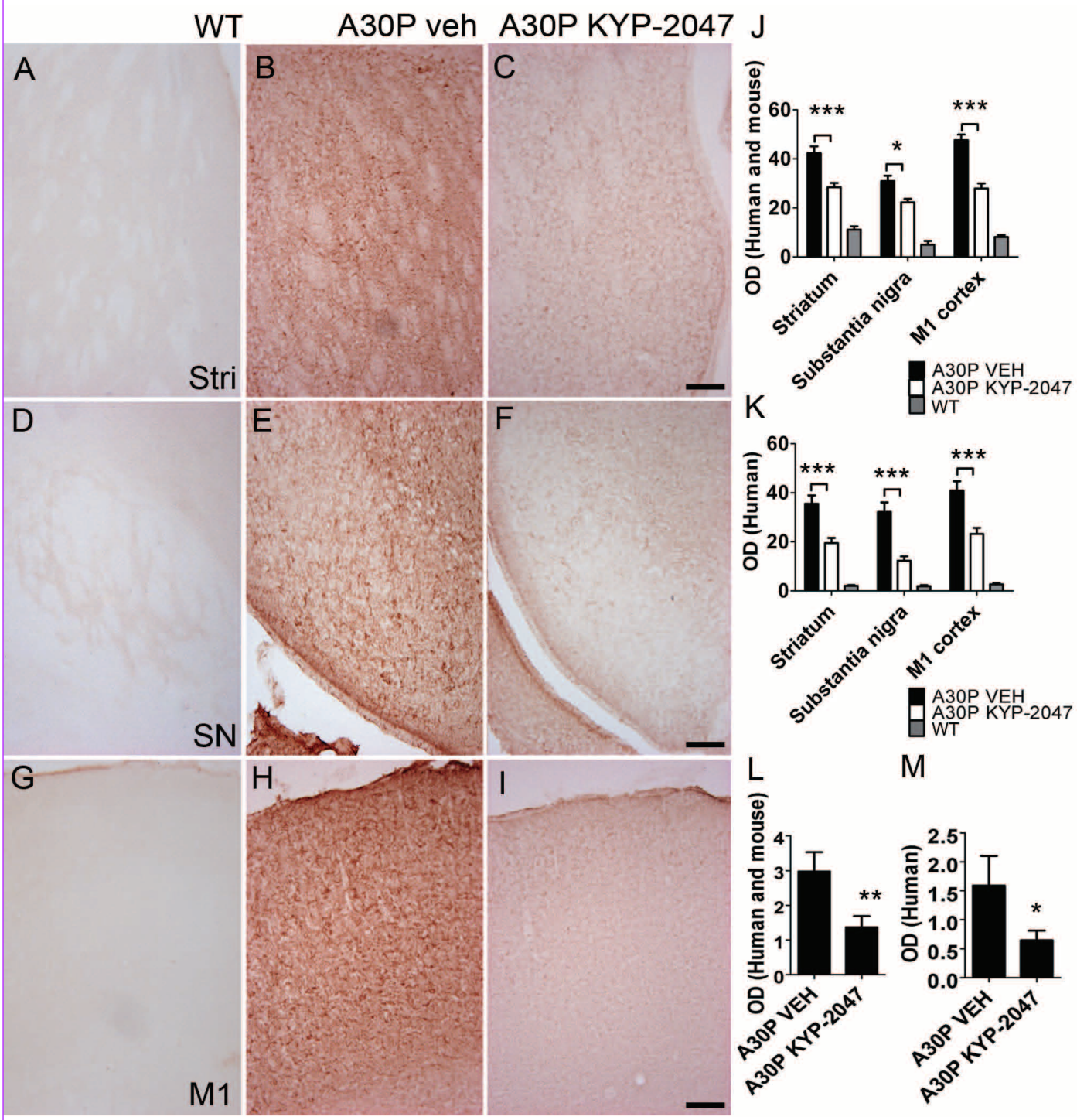
WT
A30P veh
A30P KYP-2047
J
A
B
C
Stri
OD (Human and mouse)
60
40
20
0
***
*
***
Striatum
Substantia nigra
M1 cortex
A30P VEH
A30P KYP-2047
WT
K
D
E
F
SN
OD (Human)
60
40
20
0
***
***
***
Striatum
Substantia nigra
M1 cortex
A30P VEH
A30P KYP-2047
WT
L
M
G
H
I
M1
OD (Human and mouse)
4
3
2
1
0
**
A30P VEH
A30P KYP-2047
OD (Human)
2.5
2.0
1.5
1.0
0.5
0.0
*
A30P VEH
A30P KYP-2047

Fig6

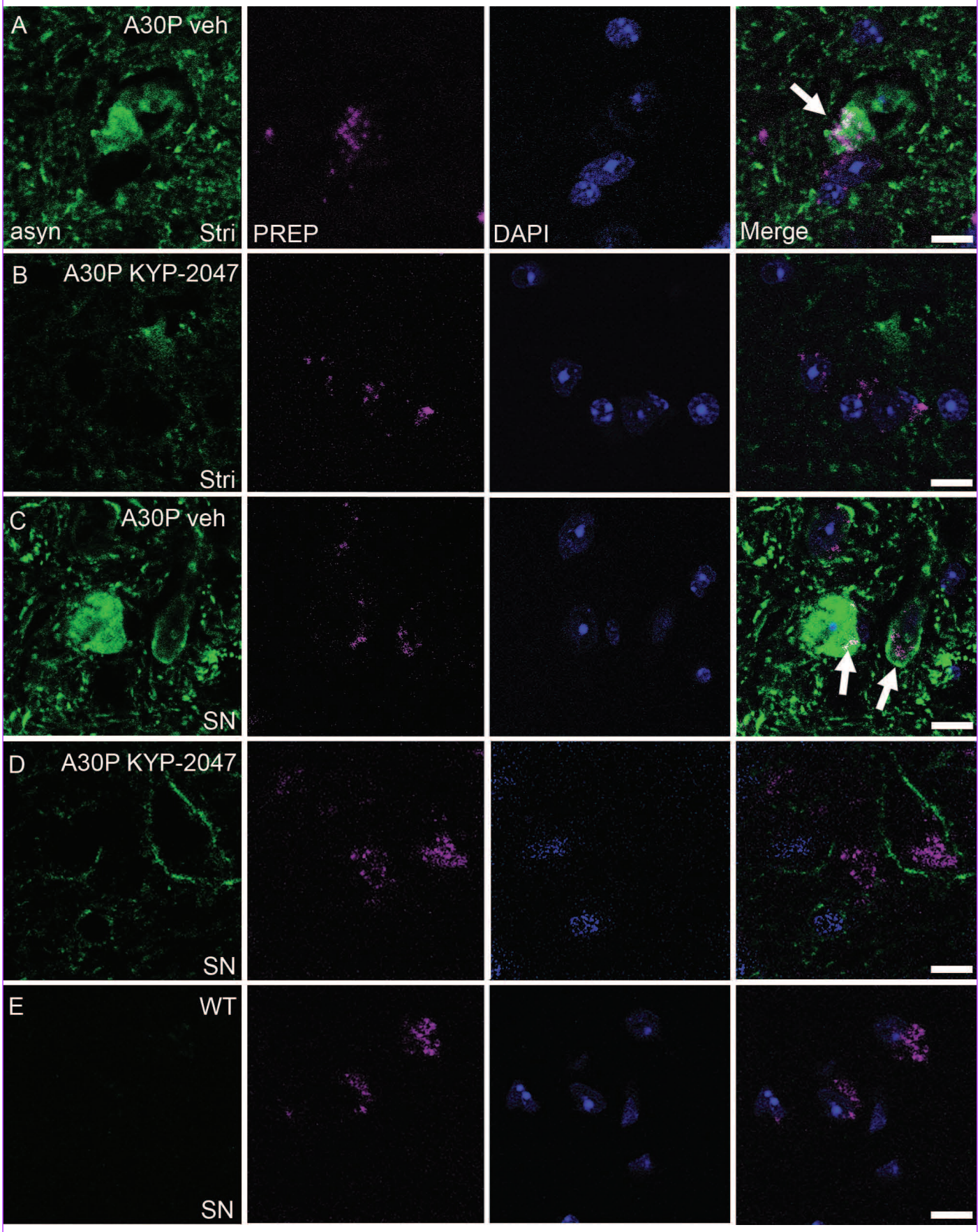
A
A30P veh
asyn
Stri
PREP
DAPI
Merge
B
A30P KYP-2047
Stri
C
A30P veh
SN
D
A30P KYP-2047
SN
E
WT
SN

Fig7